

be used. This makes the pH₂ method available for biochemical research on proton-sensitive systems.

Temperature and isotope dependence of the back-reaction confirm its diffusion-controlled mechanism. This makes the back-reaction a possible research probe for protic reaction medium properties.

Acknowledgment. This research was supported by the Israeli Commission for Basic Research and the United States-Israel Binational Science Foundation.

Registry No. D₂, 7782-39-0; BCG, 76-60-8; 8-hydroxy-1,3,6-pyrenetrisulfonate anion, 86527-89-1.

Absorption Cross Section and Kinetics of IO in the Photolysis of CH₃I in the Presence of Ozone

R. A. Cox* and G. B. Coker

Environmental and Medical Sciences Division, A.E.R.E. Harwell, Oxon OX11 0RA, England (Received: December 28, 1982)

The photolysis of CH₃I in the presence of O₃ was used as a source of IO radicals in N₂ + O₂ diluent at 1-atm pressure and 303 K. IO was detected in absorption by using the molecular modulation technique. The absorption spectrum in the region 415–470 nm, arising from the A²Π ← X²Π transition of IO, was recorded and the absolute absorption cross section at the band head of the (4–0) band at 426.9 nm determined to be $3.1_{-1.5}^{+2.0} \times 10^{-17}$ cm² molecule⁻¹. IO decayed by a rapid reaction which yielded an aerosol of probable formula I₄O₉ as final product. The observed rate coefficient for IO decay was near the gas kinetic collision rate which probably reflects an efficient attachment of IO radicals to the growing aerosol. The significance of the photochemical and kinetic parameters for atmospheric iodine chemistry is briefly discussed.

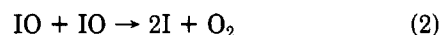
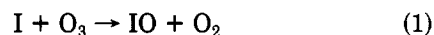
Introduction

The gas-phase chemistry and photochemistry of the halogen monoxide radicals ClO and BrO has been the subject of intense study in recent years, because of their important role in the catalytic cycles resulting in ozone destruction in the stratosphere. These XO species are rather unreactive toward stable closed-shell molecules but they undergo a variety of interesting rapid bimolecular and termolecular reactions with other odd-electron species.¹ These reactions determine the atmospheric behavior of active ClO and BrO species which are released as a result of the breakdown of Cl- or Br-containing molecules by photodissociation or free-radical attack.²⁻⁴

The chemistry of IO radicals and related I-containing species is much less well-defined. In a recent paper Chameides and Davis⁵ have suggested a possible influential role of iodine photochemistry in the budget of ozone in the troposphere, particularly in the marine boundary layer where there is a significant flux of gaseous CH₃I from the ocean to the atmosphere.⁶ In their paper Chameides and Davis⁵ have formulated the expected chemical behavior of gaseous I-containing species in the atmosphere, based largely on the analogy with ClO and BrO. Their review of the available kinetic and photochemical data revealed large gaps in knowledge but it was clear that photochemically driven cyclical reactions involving I, IO, O₃, NO_x, and HO_x could be important in the atmosphere. This arises principally because (a) the electronic absorption spectra

of most I-containing compounds extend into the intensity-abundant near-UV and visible regions of the solar spectrum and (b) the weakness of the H–I bond makes formation of relatively stable hydrogen iodide, in H-atom abstraction reactions of I atoms, very slow at prevailing atmospheric temperatures and trace gas composition.

The key iodine reactions leading to ozone destruction are as follows:



Kinetic data for these reactions have been reported by Clyne and Cruse,⁷ who used absorption in the A²Π ← X²Π electronic transition near 427 nm to monitor IO in a low-pressure flow system. They found a relatively rapid reaction of I with O₃ ($k_1 \approx 8 \times 10^{-13}$ cm³ molecule⁻¹ s⁻¹) to produce IO in both $v'' = 0$ and $v'' = 1$ vibrational levels of the ground state. The results for the decay of IO were consistent with a second-order process with a rate coefficient of $k_2 = 5.2 \times 10^{-12}$ cm³ molecule⁻¹ s⁻¹. However, the extent to which reaction 2 was occurring was not clear since O₃ was not apparently removed in the presence of IO, and wall removal of I atoms was reported to be very fast.

The A ← X transition of IO was first reported by Gaydon and co-workers,⁸ as the so-called methyl iodide flame bands; the transition has subsequently been investigated in absorption by Ramsay and co-workers^{9,10} using flash photolysis techniques. The intense absorption bands due to the vibrational ground state lie in the region 470–400 nm. Absorption in this region leads to predissociation⁹ and therefore the atmospheric photolysis of IO

(1) M. A. A. Clyne and J. A. Coxon, *Proc. Soc. London, Ser. A*, **308**, 207 (1968).

(2) R. S. Stolarski and R. J. Cicerone, *Can. J. Chem.*, **52**, 1610 (1974).

(3) Y. L. Yung, J. Pinto, R. T. Watson, and S. P. Sander, *J. Atmos. Sci.*, **37**, 339 (1980).

(4) D. L. Baulch, R. A. Cox, P. J. Crutzen, R. F. Hampson, J. A. Kerr, J. Troe, and R. T. Watson, *J. Phys. Chem. Ref. Data*, **11**, 327 (1982).

(5) W. L. Chameides and D. D. Davis, *J. Geophys. Res.*, **85**, 7383 (1980).

(6) J. E. Lovelock, R. J. Maggs, and R. J. Wade, *Nature (London)*, **241**, 194 (1973).

(7) M. A. A. Clyne and H. W. Cruse, *Trans. Faraday Soc.*, **66**, 2227 (1970).

(8) E. H. Coleman, A. G. Gaydon, and W. M. Vaida, *Nature (London)*, **162**, 108 (1948).

(9) R. A. Durie and D. A. Ramsay, *Can. J. Phys.*, **36**, (1958).

(10) R. A. Durie, F. Legay, and D. A. Ramsay, *Can. J. Phys.*, **38**, 444 (1960).

could be important. The absolute cross sections for IO have not however been determined with any certainty.⁴

In the present work the molecular modulation technique has been employed to investigate the spectrum and kinetics of the IO radical, produced in the photolysis of methyl iodide in the presence of ozone at 1-atm total pressure. Measurements of the photochemical production rate and decay kinetics of IO from time-resolved absorption in the A ← X system at 427 nm allowed determination of the absolute cross section for absorption and provided new information on the chemical behavior of IO.

Experimental Techniques

The photochemical modulation spectrometer used in this work has been described before.¹¹ The jacketed silica reaction cell was 120 cm long and had 3.0-cm i.d. with ports at both ends for introduction of gas mixtures. The radially mounted 120 cm long photolysis lamps were of two types. Quartz low-pressure mercury lamps (Philips TUV/40W) emitting mainly at 254 nm were used for CH₃I photolysis and gold fluorescent lamps (500 < λ < 700 nm, λ_{max} = 570 nm; Thorn Ltd) for I₂ photolysis. The lamps were driven by a square-wave modulated 250-V dc supply.¹² IO absorption was monitored on a collimated beam from a tungsten-halogen lamp, which traversed the long axis of the cell, before dispersion on a 0.75-m Czerny-Turner monochromator (Spex 1700) and detection on a photomultiplier. By use of a blue glass transmission filter (Chance) and fine adjustment of slit height, stray light scattered from the photolysis lamps into the detector was reduced to an acceptably low level. The spectral resolution was 0.27 nm. Spectrophotometric measurements of other species were conducted by using a deuterium lamp source (Manufacturers Supply Ltd) which was interchanged with the tungsten source. Both source lamps were operated from current-stabilized power supplies (Nortech Ltd).

Gas mixtures were prepared by flow techniques in a glass/Teflon manifold and flowed through the reaction cell at 1-atm pressure. The carrier gas was N₂ + O₂ (60:40 mole ratio) at a flow rate up to 3 L min⁻¹, and CH₃I was introduced by passing a slow flow of N₂ (0.5–2 cm³ min⁻¹) through a saturator containing pure CH₃I liquid at 273 K into the manifold. O₃ was introduced by passing pure O₂ (4–10 cm³ min⁻¹) through a silent discharge ozonator into the manifold. The flows were adjusted to give the required concentrations of CH₃I and O₃ in the range (0.2–6) × 10¹⁵ molecules cm⁻³ as measured by conventional UV spectrophotometry in the reaction cell.

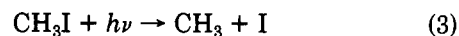
Signals arising from modulated absorption were detected by using a digital lock-in system and recorded either as in-phase and in-quadrature components of absorption, relative to the photolysis source, or as a time-resolved absorption wave form on a specially designed multichannel analyzer based on the Harwell microcomputer "MOUSE". The function of the detectors has been described elsewhere.^{11,13}

All experiments described below were conducted at a temperature of 303 K and a pressure of 1 atm.

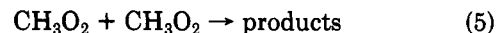
Results

Spectrum of the IO Radical in the 415–470-nm Region. IO radicals were produced by the photolysis of CH₃I (at 254 nm) or I₂ (at ~500 nm) in the presence of ozone, when

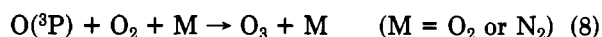
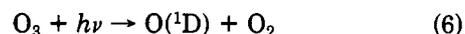
the following reactions are expected to occur, on the basis of the available literature information:



Both the ground-state I(²P_{3/2}) and excited-state I(²P_{1/2}) species can be produced in reactions 3 and 4 but rapid collisional relaxation of I(²P_{1/2}) is expected under the experimental conditions. The rapid rate of reaction 1, $k_1 = 8 \times 10^{-13} \text{ cm}^3 \text{ molecule}^{-1} \text{ s}^{-1}$, ensures that, at the O₃ concentrations used (~10¹⁵ molecules cm⁻³), IO production is fast compared to the typical modulation period of the photolysis, 0.3–1.0 s. Methyl radicals produced in reaction 3 react rapidly with O₂ to form peroxyethyl radicals, CH₃O₂, which are subsequently expected to form the organic oxidation products HCHO and CH₃OH, through the self-reaction of CH₃O₂, reaction 5, which is reasonably well



characterized.¹⁴ Photolysis of O₃ also occurs at 254 nm but the atomic O products are not expected to influence IO formation since O₃ is rapidly reformed by quenching of the excited O(¹D) atom to ground-state O(³P), followed by recombination with O₂:



The removal processes for IO in this system are discussed in the following section where the observations of the kinetic behavior of IO are considered. Observation of the modulated absorption spectrum requires only that IO be removed chemically with a time constant comparable to the modulation period. Experimentally it was found that in-phase modulated absorption in the region of the IO bands could be observed with a modulation period of 0.5 s when either I₂ or CH₃I was photolyzed in the presence of O₃. The precursor concentrations and photolysis intensity were varied to obtain optimum conditions but even at relatively high photochemical production rates (~10¹³ molecules cm⁻³ s⁻¹) only weak signals (in-phase absorption < 2 × 10⁴) were obtained, indicating that rapid chemical removal of IO occurred in this system.

For investigation of the spectrum, CH₃I was used as precursor since more random noise was encountered when I₂ photolysis was used. Typical concentrations used were [CH₃I] = 2 × 10¹⁵ molecules cm⁻³ and [O₃] = 1 × 10¹⁵ molecules cm⁻³ with 2-Hz photolysis using two lamps. In-phase and in-quadrature components at 0.1–0.25-nm intervals in the range 415–470 nm were recorded with an averaging time of 60–120 s. Data points were normalized relative to the in-phase component at 426.9 nm. The resultant spectrum illustrated in Figure 1 was obtained by three-point smoothing of over 250 data points. The absolute cross sections were based on a value of σ = 3.1 × 10⁻¹⁷ cm² molecule⁻¹ at 426.9 nm as determined in the kinetic experiments, all data being normalized to absorption at this wavelength.

Clearly defined absorption bands are evident at 419.3, 427.0, 435.7, 444.8, and 455.3 nm which can be assigned the 5–0, 4–0, 3–0, 2–0, and 1–0 bands in the A²Π ← X²Π system of IO on the basis of previous work.^{8–10} The weak

(11) R. A. Cox, R. G. Derwent, A. E. J. Eggleton, and H. J. Reid, *J. Chem. Soc., Faraday Trans. 1*, **75**, 1648 (1979).

(12) R. A. Cox and R. G. Derwent, *J. Chem. Soc., Faraday Trans. 1*, **75**, 1635 (1979).

(13) R. A. Cox, D. A. Sheppard, and M. P. Stevens, *J. Photochem.*, **19**, 189 (1982).

(14) H. Niki, P. D. Maker, C. M. Savage, and L. P. Breitenbach, *J. Phys. Chem.*, **85**, 877 (1981).

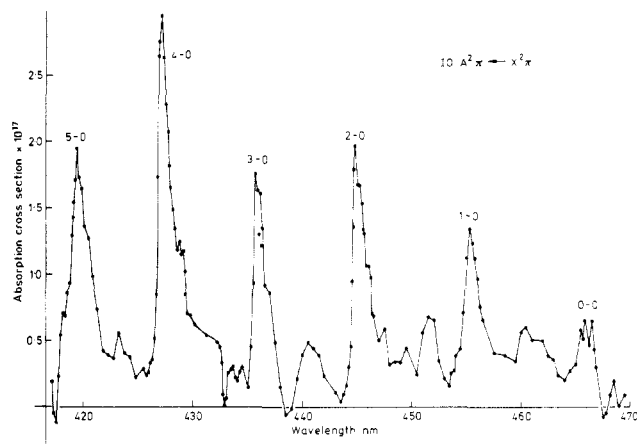


Figure 1. Molecular modulation spectrum of IO in the region of 415–470 nm obtained from 2-Hz photolysis of $\text{CH}_3\text{I}-\text{O}_3-\text{N}_2$ mixtures. Resolution = 0.27 nm. Absorption cross section relative to a value of $3.1 \times 10^{-17} \text{ cm}^2 \text{ molecule}^{-1}$ at 426.9 nm.

feature near 466 nm can be ascribed to the 0–0 band. Significantly no strong features arising from absorption from the $v'' = 1$ vibrational level of the $X^2\Pi$ ground state at 458 nm (2–1), 448 nm (3–1), could be observed in contrast to the observations of Clyne and Cruse,⁷ who employed the reaction $\text{I} + \text{O}_3$ as a source of IO in a discharge flow system at low total pressures. It is reasonable to expect rapid collisional relaxation of IO ($v'' = 1$) species at 1-atm pressure, hence, the absence of “hot” bands in the present work.

Photodissociation Rate of CH_3I . A knowledge of the photodissociation rate k_3 for CH_3I at 254 nm was necessary to determine the rate of photochemical production of IO. k_3 was determined from observation of the decay in absorption at 280 nm when static mixtures of CH_3I in $\text{N}_2 + \text{O}_2$ at 1-atm pressure were photolyzed. Figure 2 shows typical plots of log (optical density) vs. time for one- and two-lamp photolysis at 1 Hz. The plots were linear showing that CH_3I decay was first order and the following values of k_3 were obtained directly from the slopes: one-lamp photolysis, $k_3 = 0.65 \times 10^{-3} \text{ s}^{-1}$; two-lamp photolysis, $k_3 = 1.41 \times 10^{-3} \text{ s}^{-1}$. On the basis of previous work on the photooxidation of CH_3I , the CH_3 radical produced in reaction 3 is expected to form CH_3O_2 which then reacts further via reaction 5 to form HCHO and CH_3OH . HCHO absorption at 280 nm is too weak to interfere significantly with the measurement of CH_3I decay. The other major product is I_2 formed by recombination of I atoms:



Formation of I_2 was measured from the increase in absorption at 500 nm during photolysis ($\sigma(\text{I}_2) = 2.1 \times 10^{-18} \text{ cm}^2 \text{ molecule}^{-1}$ at 500 nm,¹⁵ see Figure 3. Comparison of the rate of I_2 formation with the rate of CH_3I decay ($\sigma(\text{CH}_3\text{I}) = 2.7 \times 10^{-19} \text{ cm}^2 \text{ molecule}^{-1}$ at 280 nm¹⁵) gave a quantum yield of $\Phi(\text{I}_2) = 0.49 \pm 0.05$, consistent with CH_3I dissociation exclusively via reaction 3 and removal of I via reaction 9.

Chemical Changes in the Photolysis of CH_3I in the Presence of O_3 . The chemical changes occurring in the photolysis of CH_3I in the presence of O_3 were investigated by observation of the changes in absorbance at different wavelengths in the range 500–200 nm during the photolysis of static $\text{CH}_3\text{I}-\text{O}_3$ mixtures. Data at 500 nm with and without O_3 present are shown in Figure 3. With no O_3

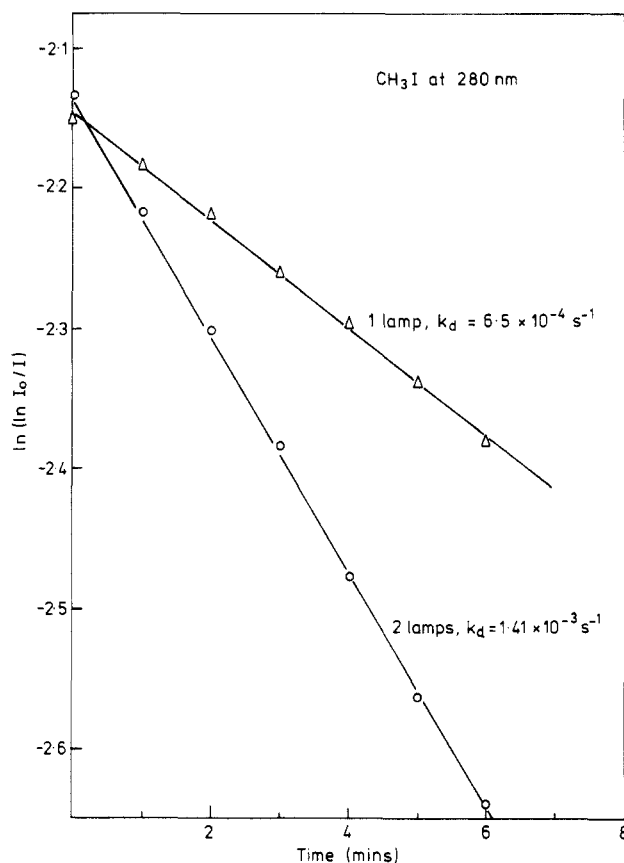


Figure 2. First-order decay in absorption at 280 nm for CH_3I photolysis at 254 nm. Photodissociation rates, k_d , determined from slope.

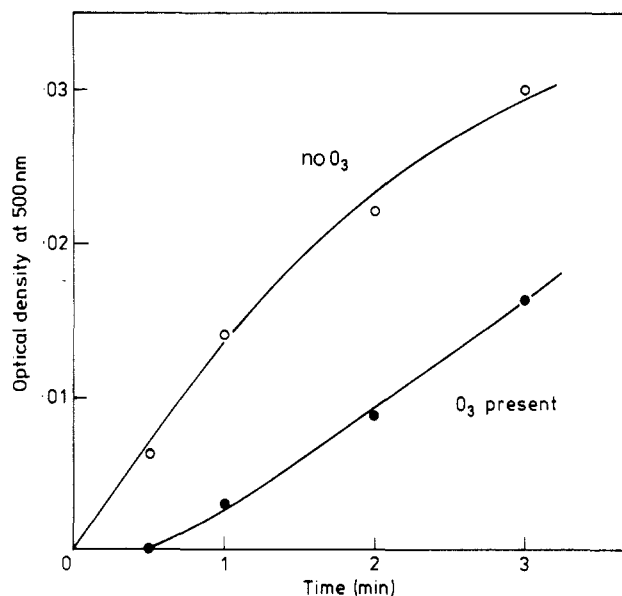


Figure 3. Changes in absorption at 500 nm in the photolysis of CH_3I at 254 nm, with and without O_3 present.

present a steady increase in absorption occurs when photolysis commences due to I_2 formation but when O_3 is present there is a distinct delay before the onset of absorption. The growth of absorption in the presence of O_3 , as measured from the change in optical density after 60-s reaction time, showed a marked increase with decreasing wavelength, as will be seen from the data in Table I. It can be concluded from these observations that I_2 is not a major product under these conditions since I_2 absorption is negligible at $\lambda < 430 \text{ nm}$.

At 261 nm, absorption decreased with time due to consumption of CH_3I and O_3 , which both have absorption

(15) J. G. Calvert and J. N. Pitts, “Photochemistry”, Wiley, New York, 1966.

TABLE I: Product Absorption in Photolysis of CH₃I + O₃ Mixtures^a

λ , nm	optical density after 60-s photolysis (1 Hz)	λ , nm	optical density after 60-s photolysis (1 Hz)
500	0.0275	261	-0.129
400	0.0625	220	0.313
300	0.242		

^a [CH₃I]₀ = 2.26 × 10¹⁵; [O₃]₀ = 0.68 × 10¹⁵ molecules cm⁻³.

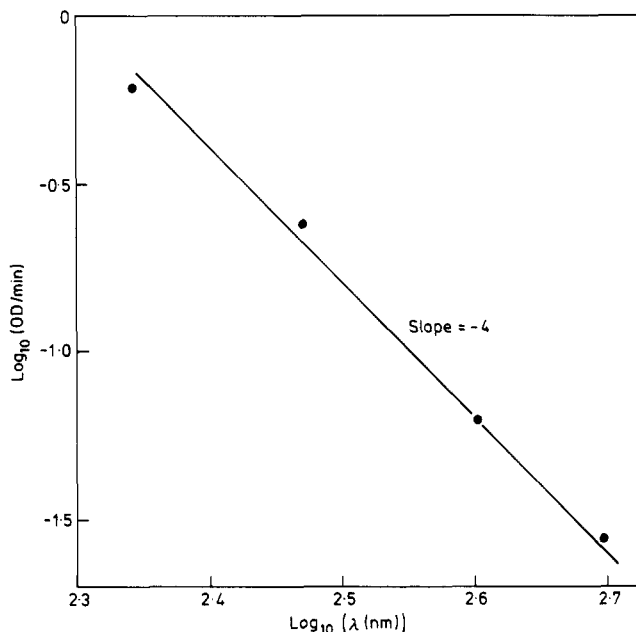


Figure 4. Plot of log (optical density) against log (wavelength) after 60-s photolysis of a CH₃I-O₃ mixture containing initially 2.3 × 10¹⁵ molecules cm⁻³ CH₃I and 0.68 × 10¹⁴ molecules cm⁻³ of O₃.

maxima at this wavelength. At 220 nm absorption increased again, indicating an even stronger product absorption than at 300 nm. The wavelength dependence of the product absorption and the nonlinear growth is indicative of the formation of a light-scattering aerosol product. In order to test this possibility the optical density changes after 60-s photolysis were plotted against wavelength as logarithmic functions. The plot is illustrated in Figure 4 and shows a linear relationship with a slope of -4. This is the expected functional relationship for extinction due to scattering by particles with radius $r \ll \lambda$, i.e., $\ll 0.2 \mu\text{m}$, according to the Rayleigh equation.¹⁶

The absorption due to aerosol product at 261 nm was determined by interpolation on Figure 4 and this allowed evaluation of the reduction in absorption due to O₃ at this wavelength, after an additional small correction for CH₃I decay. The rate of loss of O₃ could then be determined ($\sigma(\text{O}_3) = 1.1 \times 10^{-17} \text{ cm}^2 \text{ molecule}^{-1}$) and comparison with the rate of CH₃I photolysis gave a quantum yield for O₃ decay of $\Phi(-\text{O}_3) = 2.1 \pm 0.2$. Since the organic species CH₃, CH₃O₂, HCHO, CH₃OH are not expected to react with O₃ under the conditions of these experiments, these results are consistent with the removal of slightly more than two O₃ molecules by each I atom produced in reaction 1. The oxide I₄O₉, a yellow solid, has been identified as a product of the reaction of I₂ in ozonized oxygen¹⁷ and in corona-discharged CH₃I-air mixtures.¹⁸ In the latter work the

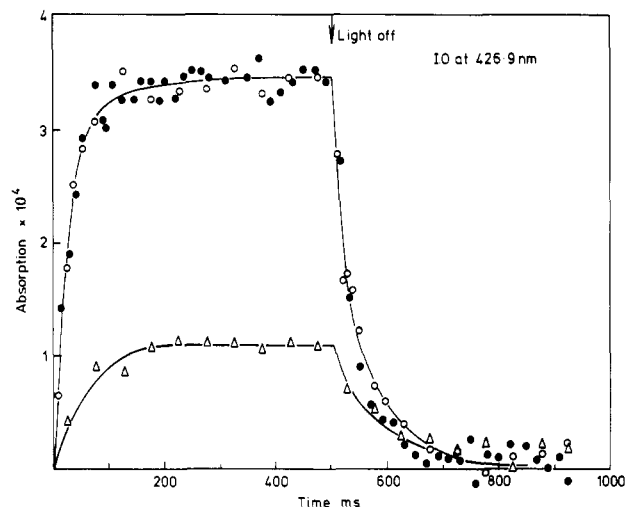
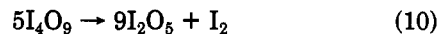
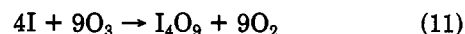


Figure 5. Time dependence of IO absorption in 1-Hz photolysis of CH₃I-O₃ mixtures: (O, ●) [CH₃I] = 2.0 × 10¹⁵ molecules cm⁻³, [O₃] = 1.57 × 10¹⁵ and 0.46 × 10¹⁵ molecules cm⁻³, respectively; (Δ) [CH₃I] = 0.32 × 10¹⁵, [O₃] = 0.48 × 10¹⁵ molecules cm⁻³. Two-lamp photolysis.

thermal behavior of the iodine oxides produced was investigated by using thermogravimetry and differential thermal analysis. Amorphous forms of I₂O₄ and I₄O₉ were characterized, the latter decomposing at 460 K according to the equation



Formation of I₄O₉ in the present system would be consistent with the overall reaction stoichiometry



The additional observation of a pale yellow deposit on the reaction cell surfaces, which decomposed slowly over extended periods to give I₂ vapor, is also consistent with this being a major product.

Kinetic Behavior of IO in the Photolysis of CH₃I-O₃ Mixtures. The kinetic behavior of IO was determined from measurement of the time-resolved absorption changes at 426.9 nm during a modulated photolysis cycle at either 1 or 2.8 Hz. Flowing mixtures of CH₃I + O₃ in N₂ + O₂ (50:50) at 1 atm were used and in a typical experiment data were collected for 30–60 min to obtain sufficient signal/noise ratio for useful analysis. The signals contained, in addition to IO absorption, changes in transmitted light due to production and removal (due to flow out) of aerosol. These were corrected assuming that aerosol scattering followed the photochemical production with zero time lag; i.e., it followed a triangular wave form oscillating about a mean value corresponding to the average extinction along the cell length. Deviation from this approximation could have led to significant error in the observed rise and decay profile for IO, particularly at high reaction fluxes when aerosol signal was relatively large. It should not, however, have influenced the measured steady-state IO absorption.

Figure 5 shows typical corrected absorption time profiles for IO in 1-Hz photolysis using different O₃ concentrations and photolysis rates. It will be seen that IO rises rapidly to a steady state during the "light-on" period and decays rapidly to a low value in the dark. The data at the higher photolysis rate shows that the steady-state absorption and the rise and decay profile were unaffected by a 3-fold

(16) Lord Rayleigh, *Philos. Mag.*, 47, 375 (1899).

(17) F. W. Cotton and G. Wilkinson, "Advanced Inorganic Chemistry", 2nd ed., Wiley-Interscience, New York, 1966, p 567.

(18) A. Wikjord, P. Taylor, D. Torgerson, and L. Hachkowski, *Thermochim. Acta*, 36, 367 (1980).

(19) M. A. A. Clyne and J. A. Coxon, *Proc. R. Soc. London, Ser. A*, 303, 207 (1968).

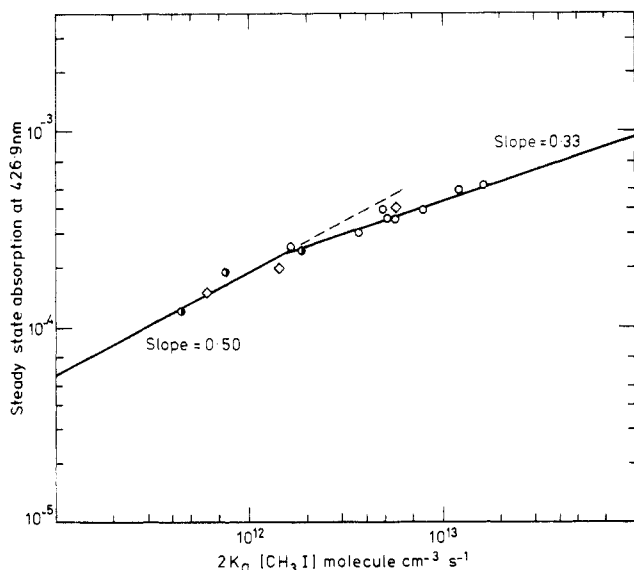


Figure 6. Plot of steady-state IO absorption at 426.9 nm against the rate of photolysis of CH_3I , i.e., $2K_d[\text{CH}_3\text{I}]$.

variation in $[\text{O}_3]$ at constant photolysis rate, $B = 2k_3[\text{CH}_3\text{I}]$. This indicates that reaction of IO with O_3 is not important in this system. The steady-state absorption, A_{ss} , showed a marked increase with photolysis rate although it was not directly proportional to B . The following general equation describes the time dependence of IO during photolysis:

$$d[\text{IO}]/dt = B - k[\text{IO}]^n \quad (\text{I})$$

where n is the order of reaction and k is the decay coefficient. The steady-state solution gives

$$A_{ss} = \sigma l[\text{IO}]_{ss} = \{B/k\}^{1/n} \quad (\text{II})$$

Figure 6 shows a log-log plot of A_{ss} vs. B for a 50-fold variation of B . The plot showed curvature with a slope ($=1/n$) decreasing from 0.5 at low B to ~ 0.3 at the higher values, indicating an increase in kinetic order from 2 to 3.

Further information concerning the kinetic behavior of IO can be obtained from the half-time for rise to and fall from the steady state, $t_{1/2}(\text{rise})$ and $t_{1/2}(\text{fall})$, and their dependence on B . Integration of the rate equation gives the following relationships:

for $n = 1$

$$t_{1/2}(\text{rise}) = t_{1/2}(\text{fall}) = \ln 2/k \quad (\text{III})$$

for $n = 2$

$$t_{1/2}(\text{rise}) = \frac{\ln 3}{2} \frac{1}{(Bk)^{1/2}}$$

$$t_{1/2}(\text{fall}) = 1/(Bk)^{1/2} \quad (\text{IV})$$

for $n = 3$

$$t_{1/2}(\text{rise}) = 0.52/(B^{2/3}k^{1/3})$$

$$t_{1/2}(\text{fall}) = 1.5/(B^{2/3}k^{1/3}) \quad (\text{V})$$

Examination of Figure 5 shows that, at the higher photolysis rate, the half-times for rise and fall to and from the steady state are approximately equal at 25 ± 5 ms. This indicates $n = 1$, i.e., first-order kinetic decay with $k = 28 \text{ s}^{-1}$. At the lower photolysis rate the rise and fall to and from the steady-state value were slower and also $t_{1/2}(\text{rise})$ ($=45 \pm 5$ ms) was significantly shorter than $t_{1/2}(\text{fall})$ ($=70 \pm 5$ ms). This indicates that IO kinetics

approximate to second order ($n = 2$) at low B which is consistent with the analysis according to eq II. At high B the kinetics are evidently complex. The apparent higher order ($n \approx 3$) from analysis by eq II could result if the decay constant k increases with increasing photolysis rate, i.e., $k = k'B^m$ and

$$A_{ss} = [B^{(1-m)/n} / (k')^{1/n}] \quad (\text{VI})$$

This situation could arise if IO reacts with a reaction product which builds up as the reaction mixture flows through the vessel. As B increases, the average amount of product in the vessel and hence average k increase. Qualitative support for this explanation comes from the observation that the values of $t_{1/2}$ at a given B increased when the total reaction time was decreased by increasing the total flow rate. The major product in this system is believed to be an aerosol with a chemical composition corresponding to $(\text{I}_4\text{O}_9)_n$. Particle growth could occur by attachment of IO molecules to existing nuclei and the kinetic behavior in such a system is expected to be complex since the physical characteristics of the aerosol will change as the reaction progresses. However, in the initial stages of the reaction the formation of particles could be initiated by bimolecular association of IO:



At low $[\text{IO}]$ and low particle density, this process could be rate determining for removal of IO and hence account for the approximate second-order kinetic behavior at low B . This explanation cannot be fully tested with the available data since (a) the IO concentration-time behavior reflects a changing chemical environment along the reaction cell, (b) the absorption signals are relatively small and subject to considerable statistical uncertainty, and (c) approximations made in correcting the absorption measurements for aerosol scattering could lead to small errors in the time resolution of IO behavior, particularly at high photolysis rates, when the correction was larger relative to the IO signal.

Since the data at low photolysis rates gave a reasonable approximation to second-order kinetics, analysis of this data was conducted to determine k^{II} , the overall second-order rate coefficient as defined by eq I where $k = k^{\text{II}}$ and $n = 2$, and to determine the absorption cross section for IO at 426.9 nm.

The slope of a plot of the steady-state IO absorption for experiments with $B < 2 \times 10^{12}$ molecules cm^{-3} against $B^{1/2}$ gave the quantity

$$\sigma / (k^{\text{II}})^{1/2} = (1.5 \pm 0.3) \times 10^{-12} \text{ cm}^{1/2} \text{ molecule}^{-1/2} \text{ s}^{1/2}$$

Integration of eq I for $n = 2$ gives the following equation describing the decay of IO in the absence of photochemical production ($B = 0$):

$$1/A - 1/A_{ss} = (k^{\text{II}}/\sigma l)t \quad (\text{VII})$$

Figure 7 shows a plot of selected data according to eq VII. The plots were linear for the first 150 ms but showed upward curvature at higher decay times (not shown). The slope in the linear region gives k^{II}/σ directly ($l = 120$ cm) and the average value obtained from these and other data was

$$k^{\text{II}}/\sigma = (1.3 \pm 0.3) \times 10^7 \text{ cm s}^{-1}$$

The following values of k^{II} and σ can then be obtained from the above measurements:

$$k^{\text{II}} = 4.0_{-2.0}^{+2.8} \times 10^{-10} \text{ cm}^3 \text{ molecule}^{-1} \text{ s}^{-1}$$

$$\sigma(426.9 \text{ nm}) = 3.1_{-1.5}^{+2.1} \times 10^{-17} \text{ cm}^2 \text{ molecule}^{-1}$$

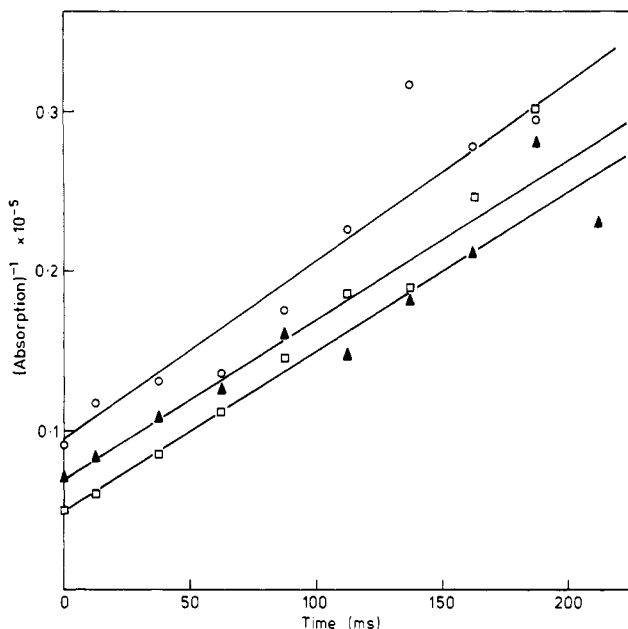
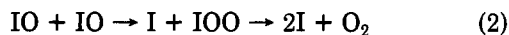


Figure 7. Plot of $(\text{IO absorption at } 426.9 \text{ nm})^{-1}$ against time following cessation of photolysis in the modulated photolysis of $\text{CH}_3\text{I} + \text{O}_3$ mixtures.

Discussion

The only previously reported kinetic data for the IO + IO reaction are those of Clyne and Cruse,⁷ who studied the reaction in a low-pressure discharge flow system using absorption in the 4-0 band to monitor IO produced in the $\text{I} + \text{O}_3$ reaction, as in the present study. They obtained $k_2/\sigma = 1 \times 10^6 \text{ cm s}^{-1}$ for the second-order decay of IO in the presence of excess O_3 , i.e., approximately a factor of 13 lower than obtained in the present work for k^{II}/σ . This difference is much larger than can be accounted for by the stated experimental uncertainties in both studies and the lower spectral resolution (0.5 nm) used in the low-pressure study possibly giving rise to a lower value for σ . It appears therefore that different elementary processes may be operative in the IO + IO reaction in the two systems. Although the kinetic behavior of IO in the present work was not strictly second order for all conditions, it is clear that the overall removal of IO, in what appears to be an association reaction, is much more rapid at 1-atm pressure than the overall decay at low pressure observed by Clyne and Cruse. The value of $k^{\text{II}} = 4.0 \times 10^{-10} \text{ cm}^3 \text{ molecule}^{-1} \text{ s}^{-1}$ at 1 atm is close to the collision rate and is therefore unlikely to apply to a bimolecular metathesis reaction which was suggested for the IO + IO reaction at low pressure:



The maximum rate coefficient for reactions of this type is of the order of $10^{-11} \text{ cm}^3 \text{ molecule}^{-1} \text{ s}^{-1}$. Furthermore, in the presence of excess O_3 this reaction would not give net removal of IO since it would be rapidly regenerated in the fast $\text{I} + \text{O}_3$ reaction. If k^{II} applies to a three-body recombination reaction



the equivalent termolecular rate coefficient for $\text{M} = \text{N}_2$ is $2 \times 10^{-29} \text{ cm}^6 \text{ molecule}^{-2} \text{ s}^{-1}$. This is approximately a factor of 15 higher than the maximum theoretical termolecular collision frequency at 298 K and in order to account for such high rates a "chaperone" mechanism has to be invoked, in which IO molecules form a loose complex with other molecular species, e.g., O_2 , thereby enhancing the apparent three-body rate coefficient. Alternatively the presence of aerosol particles may play a role in enhancing

TABLE II: Atmospheric Photolysis Rates of IO Radical

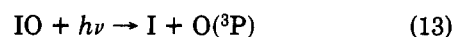
λ , nm	$10^{17}\sigma$, $\text{cm}^2 \text{ molecule}^{-1}$	$10^{-14}I_\lambda$, ^a photons $\text{cm}^{-2} \text{ s}^{-1}$	$10^3 I_\lambda \sigma \lambda$, s^{-1}
470-465	2.79	5.39	15.0
465-460	4.21	5.39	22.7
460-455	10.0	5.27	52.7
455-450	3.98	5.27	9.3
450-445	14.10	4.64	65.4
445-440	3.09	4.64	14.3
440-435	10.20	3.99	40.7
435-430	2.86	3.99	11.4
430-425	16.40	3.87	63.5
425-420	9.30	3.87	36.0
420-415	8.40	1.96	16.5
			$\Sigma = 0.3 \text{ s}^{-1}$

^a At $Z = 40$. Z = solar zenith angle.

the decay rate of IO, but it is not possible to formulate a realistic quantitative model on the basis of the experimental observations. The available evidence does not therefore allow any definite conclusion regarding the elementary steps involved in the IO + IO reaction at either high or low pressures.

The value obtained for the absorption cross section at 426.9 nm, $\sigma = 3.1 \times 10^{-17} \text{ cm}^2 \text{ molecule}^{-1}$, is also considerably greater than the value suggested by Clyne and Cruse,⁷ $\sigma = 5 \times 10^{-18} \text{ cm}^2 \text{ molecule}^{-1}$. However, they were unable to obtain a definitive measurement in their system. It is of interest to compare the present value with those for the strongest bands in the $\text{A}^2\Pi \leftarrow \text{X}^2\Pi$ systems for BrO and ClO measured at comparable spectral resolution, $10^{17}\sigma = 1.8$ (338.3 nm)¹³ and 0.72 (277.2 nm),¹⁹ respectively. There appears to be a trend of decreasing absorption strength in the halogen series.

We believe that the value of $\sigma(\text{IO})$ at 426.9 nm obtained in this work provides a reasonable basis for determination of the integrated absorption coefficients for IO over the whole band system for the purposes of calculation of the photodissociation rate of IO in the atmosphere. Since the high-resolution spectrum of IO determined by Durie and Ramsay⁹ exhibits strong predissociation, it can be safely assumed that dissociation via the overall reaction



occurs with unit quantum efficiency in the $\text{A} \leftarrow \text{X}$ system. The photodissociation rate is then given by a summation of the product of the absorption cross section and the solar intensity, I_λ

$$k_{13}(\text{s}^{-1}) = \sum_{\lambda} \Phi \sigma_{\lambda} I_{\lambda} \quad (\Phi = 1)$$

where σ_{λ} and I_{λ} are average values over an appropriate wavelength interval. Table II shows values of σ averaged over 5-nm intervals based on the data in Figure 1, together with I_{λ} values²⁰ for a solar zenith angle of 40° , averaged over the same wavelength interval, and the product $\sigma_{\lambda} I_{\lambda}$. The summation gives $k_{13} = 0.3 \text{ s}^{-1}$ for this sun angle implying a lifetime of $\sim 2 \text{ s}$ for IO with respect to photodissociation.

The formation of a light-scattering aerosol has not been previously reported either in the flash photolysis⁹ investigation of IO or in the low-pressure discharge flow study.⁷ In the latter study however it was noted that a solid deposit formed on the flow tube walls downstream of the $\text{I} + \text{O}_3$ reaction zone. In the present work diffusion to the wall would be slow at 1-atm pressure and conditions are

(20) J. P. Peterson, EPA Report 600/4-76-025, U.S. EPA, Research Triangle Park, NC, June 1976.

therefore favorable for aerosol formation.

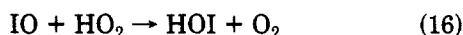
The formation of aerosol in the present system is believed to occur by nucleation in the initial stages followed by rapid condensation of IO_x material onto the nuclei leading to growth to light-scattering size. The observed light scattering after 10-s reaction time corresponds approximately to $\eta \simeq 5 \times 10^5$ particles cm⁻³ of radius $r = 0.1$ μ m, and growth by coagulation would be 2 orders of magnitude too slow to achieve this population. The mass concentration corresponds well with the total IO flux ($\sim 3 \times 10^{12}$ molecules cm⁻³ s⁻¹) if the particle density is ~ 4 g cm⁻³. The rate of attachment of gaseous species to this aerosol, as calculated from the modified Fuchs equation^{21,22}

$$k = \frac{1}{C} \frac{dc}{dt} = 4\pi r^2 \eta N \alpha$$

$$C = [\text{IO}] \quad N = [RT/(2\pi M)]^{1/2}$$

is $k = 2.5\alpha$ s⁻¹, where α is the attachment efficiency. Therefore, even with $\alpha = 1$, this process could only give an effective first-order attachment to $\alpha = 1$, this process could only give an effective first-order attachment to the aerosol rate of ~ 2.5 s⁻¹. Typical observed removal loss rates for IO radicals were at least a factor of 10 higher than this. A larger number of smaller particles would need to be present to account for the observed removal of IO by attachment to the aerosol. Further investigation of this nucleation/coagulation process would be of some interest.

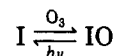
Behavior of IO in the Atmosphere. According to current ideas regarding the gas-phase reactions of IO, its removal pathways in the atmosphere involve photodissociation (reaction 13) and reaction with NO, NO₂, and HO₂ (reactions 14–16, respectively). Typical daytime concentrations



of the reaction partners in the boundary layer over land are 1 ppb NO, 3 ppb NO₂ and 0.01 ppb HO₂. Taken with a recent measured value of $k_{14} = 1.7 \times 10^{-11}$ cm³ molecule⁻¹ s⁻¹,²³ current estimates⁵ of the rate constants k_{15} and k_{16} give effective first-order loss rates of IO of 0.5, 0.3, and 0.001 s⁻¹, respectively. The present work gives a value of 0.3 s⁻¹ for the dissociation reaction 13 which makes this route competitive with the important reaction with nitrogen oxides. In remote land areas and over oceans, where NO and NO₂ concentrations are believed to be much lower,

photolysis by reaction 13 may be the major process converting IO to I. A previous estimate⁵ of the daytime average value of k_{13} gave a value approximately a factor of 10 lower than the present value.

The interconversion of I and IO in the sunlit atmosphere is so rapid that, in the absence of NO_x species, the following equilibrium will be maintained:

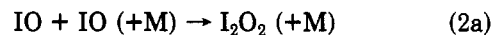


with $[\text{I}]/[\text{IO}] = k_6/k_5[\text{O}_3] \simeq 0.38$ for $k_{13} = 0.3$ s⁻¹ and $[\text{O}_3] = 40$ ppb. When NO₂ is present at the ppb level, IO (and I) will be fairly rapidly converted to iodine nitrate, which appears to be the main homogeneous removal pathway, although firm experimental data on the formation and fate of this substance are lacking. The present work indicates a rather strong tendency for IO to attach the aerosol particles, implying a potential heterogeneous removal pathway for I and IO that may also be important.

The reaction



is also considered to be important in the atmosphere, since it recycles IO to I without accompanying production of O(³P) or O₃. Chameides and Davis⁵ have indeed suggested that catalytic O₃ removal resulting from this reaction, coupled with the I + O₃ reaction, could account for the very low O₃ mixing ratios observed in tropical oceanic surface air. We were unable to see any evidence of this reaction in the present work where the recombination of IO radicals to give higher oxide products was apparently 10–100 times faster than the value of k_2 suggested by Clyne and Cruse.⁷ If this truly reflects a change in mechanism of the elementary IO + IO reaction in going from a few torr to 1-atm pressure, then mutual recombination of IO, for example, by



could also provide a significant atmospheric sink for IO and hence for other iodine species which form IO following photodissociation. Ozone removal by iodine species would in this case be much less important. Further work on the kinetics and mechanism of IO removal in the presence of O₃, in particular its pressure dependence, is clearly desirable.

Acknowledgment. Thanks are due to J. A. Garland and R. G. Derwent for helpful discussions regarding this work. The experiments involving I₂ photolysis were performed by T. J. Wallington, University of Oxford, while attached to AERE.

Registry No. O₃, 10028-15-6; I, 14362-44-8; MeI, 74-88-4; IO, 14696-98-1.

(21) A. C. Chamberlain, A. E. J. Eggleton, W. J. Megaw, and J. B. Morris, *Discuss. Faraday Soc.*, **30**, 1 (1960).

(22) J. A. Garland, *J. Nucl. Energy*, **21**, 687 (1967).

(23) G. Ray and R. T. Watson, *J. Phys. Chem.*, **85**, 2955 (1981).